Republic of Iraq
Ministry of Higher Education and Scientific Research
University of Babylon
College of Sciences for Women
Department of Laser Physics

Thermoelectric and Optical Properties of Nano Molecular Junctions

A Thesis

Submitted to the Council of the College of Sciences for Women,

University of Babylon

In Partial Fulfillment of the Requirements for the Degree of

Master in Laser Physics and its Applications

By

Marwaa Abdulhussien Kadhim

(B.Sc. 2016)

Supervised by

Assistant. Prof. Dr. Oday A. Al-Owaedi

1443 A.H. **2022 A.D.**

بِسْمِ اللَّهِ الرَّحْمَٰنِ الرَّحِيمِ

﴿إِنَّا لَا نُضِيعُ أَجْرَ مَنْ أَحْسَنَ عَمَلًا﴾

صدق الله العليُّ العظيم

ايه 30

سورة الكهف

Dedication

This thesis is dedicated to

My parents who have provided me with confidence and support

My brothers and sisters whose love motivated me to challenge myself and to work harder

My husband for his understanding and enduring patience and encouragement through this hard work.

To my friends and colleagues who helped me

Marwaa

Acknowledgment

This thesis would never completed without the excellent supervision and guidance I received from Assistant Prof. Dr. Oday A. Al-Owaedi. There are no words in English books can express my gratitude to you. Really you were excellent supervisor.

Also I would like to pay my regards to all relatives and friends for the help they showed at the Department of Laser Physics.

Also my very deep respect and sincere appreciation to my family, whose patience and moral encouragement gave me so much hope and support.

Above all, my great thanks to **ALLAH** for his mercy and blessing.

Abstract

Quantum interference (QI) is one of the most fundamentals science, which can be a powerful strategy to control and enhance the electric, thermoelectric and spectral properties of single molecules. Here, the density-functional-theory-based quantum transport calculations have been used to figure out the electrical conductance (G/G_0), which supplies unique understanding into the thermopower (S) and emission oscillator strength (f_{em}) of from a series of oligophenylene-ethynylene (OPE) derivatives with thiol end-groups, and para or meta transport connections, which underpins their spectral and heat transport properties. The molecules with meta connection (OPE-4,5,6) demonstrated the signature of a destructive quantum interference, which resulted to a low conductance (0.65×10^{-4}, 0.5×10^{-6}, and 0.17×10^{-6}) respectively produce a high thermopower (165, 182, and 266 μVK^{-1}). These structures yield very low emission oscillator strength (0.96, 0.75, and 0.66) respectively. In contrast, the para linking in molecules OPE-1,2,3 led to a constructive quantum interference, which was the reason for the high conductance (0.52×10^{-3}, 0.88×10^{-3}, and 0.22×10^{-2}) respectively. These molecule exhibited a low thermopower (22, 21, and 13), and a high emission oscillator strength (2.15, 2.15, and 2.03) respectively. Finally, the

properties of all molecules studied here are dominated by the highest occupied molecular orbital (HOMO) level.

Table of Contents

Chapter 1: Introduction

Chapter 2: Density Functional Theory and Transport Calculations

List of Figure

List of Table

List of Abbreviations

Abbreviation	Physical meaning
DFT	Density functional theory
UV	Ultra-Violet
Vis	Visible region
NIR	Infrared Nuclear
HOMO	High occupied molecular orbitals
LUMO	Lowest unoccupied molecular orbitals
TD-DFT	Time dependent Schrödinger equation
SIESTA	Spanish Initiative for Electronic Simulations with Thousands of Atoms
KS	Kohn and Sham
LDA	Local density approximation
GGA	Generalized gradient approximation
CA	Ceperly and Alder
PZ	Perdew and Zunger
PBE	Perdew, Burke and Ernzherhof
LCAOBs	Linear Combination of Atomic Orbital Basis set
BSSE	Basis set superposition error correction
CP	Counterpoise Correction

DOS	Density of states
QI	Quantum interference effect transistors
HK	Hohenberg-Kohn-Sham
NEGF	Non-equilibrium Green's function
B_3LYP	Becke 3 (Lee-Yang-Parr)
SZ	Single zeta
DZ	Double zeta
SZP	Single zeta polarized
DZ	Double zeta polarized

Chapter One

Introduction

Chapter1: Introduction

1.1. General Introduction

In the mid-1960s, Gordon Moore observed that the number of transistors per unit area on a chip was doubling approximately once every two years [1]. He modestly speculated that this trend could continue for a further ten years, but nearly half a century later, the exponential growth continues. However, if Moore's law is to continue, the transistors will have to shrink to atomic scale within twenty years and enter the field of nanoelectronics. Recently, new insights in the field of nanoscience have been obtained from the application of fundamental modeling techniques such as density functional theory (DFT), and molecular dynamics [2]. Advances in computer technology have led to an increase in computational capability which has made possible the modeling and simulation of complex systems with millions of degrees of freedom. However, the full potential of novel theoretical and modeling tools has not been reached yet.

Chapter1: Introduction

1.2. Oligo(phenylene-ethynylene) Molecules

The myriad of wirelike molecules that have been prepared and studied in thin film and single-molecule junctions, the oligo(phenylenevinylene) and oligo(phenyleneethynylene) (OPE) occupy a particularly prominent position [3]. The ease of synthesis, stability under ambient conditions, ready functionalization with a wide range of electronically and sterically interesting groups, and suitability to form modular structures of regularly increasing length have made these systems idea workhorses for the explorations of electronic phenomena in molecular systems[4,5]. There are many reviews and discussion papers that address the chemistry and junction characteristics of these species [6], a comprehensive description of this molecular class alone would occupy at least an entire volume. The OPE backbone is thought to offer a wider range of conformations, given the essentially barrierless rotation of the phenylene moieties around the ethynyl axis [7], the great advantage of this fragment is the (relative) simplicity of synthetic approach based on sequential and convergent crosscoupling methods [8].

In fact, Oligo(phenylene-ethynylene) (OPE) compounds represent a particular unique family of molecular wires. They are fully π-conjugated rigid rod-like molecules with a HOMO−LUMO gap of ∼3 eV [9 – 10].

Chapter1: Introduction

1.3. Single Molecule Junctions

Due to the intrinsic limitations of silicon-based electronics, the idea of using organic molecules as functional units in electronic devices has received increasing interest [11]. The detailed understanding of charge transport through single-molecule junctions is a key prerequisite for the design and development of molecular electronic devices. The implementation of single molecules and tailored molecular assemblies in electronic circuits requires the optimization of their structures toward desired functionalities and a reliable method of wiring them into nanoscale junctions [12−13].

In recent years, important correlations between transport properties and molecular structure have been demonstrated from the investigation of functional properties of single molecules and self-assembled monolayers [14−15]. Examples of reported functionalities illustrated by single molecules include diodes, [16−17] transistors,[18,19] memory effects, [20−21] and various switching phenomena, such as processes triggered by an electric potential, [22,23], the mechanical motion of a probe electrode, [24], or light excitation [25,26,27]. Furthermore, molecular wires are essential structures for connecting functional units [28, 29].

Chapter1: Introduction

1.4. Literature Review

[1] *Oday A. Al-Owaedi et al*, in 2015, have presented charge transport studies of pyridyl terminated OPE derivatives, using the MCBJ and STM-BJ techniques, DFT-based theory and analytic Green's functions, and have investigated the interplay between QI effects associated with entral and terminal rings in molecules of the type X-Y-X. *Julia Ponce et al* in 2016, have performed the spectroscopic measurements and DFT calculations of OPE molecular junctions, and their studies suggest that the room-temperature emission of the iridium complexes can be unambiguously assigned to 3 metal-to-ligand charge-transfer excited states in all cases[30].

[2] *Subodh P. Jagtap et al* in 2017, have studied experimentally and theoretically that the absorption and emission spectra of the stacked OPE compounds and compared them to those of the individual unstacked oligomers. These optical studies, when analyzed together with the results of TD-DFT calculations, clearly demonstrate the effect of interchain interactions on the low energy photophysics of stacked compounds[31].

[3] *Yuqing Liu et al* in 2018, have fabricated a high quality SAMs based on OPE3 and OPE3-TTF with diamine anchoring groups were grown on the Au substrate. They found the molecular conductance of diamine

OPE3 was markedly increased by TTF group and the conductance differences were 17 and 46 times for Au and Pt tips[32].

[4] *L. Herrer et al* in 2019. They have explored the characteristics of molecular single and large molecules, and they found a double anchor group, formed from 2-aminepyridine reveals a conductance value one order of magnitude larger than state-of-the-art monodentate materials of OPE derivatives with the same molecular structure. Their studies also confirm that the lowest conductance value was presented by a single molecule, while the highest one from the monolayer molecule[33].

Hang Chen et al in 2020, have studied the thermoelectric properties of OPE derivatives using a modified STM-BJ technique, and they demonstrated the importance of the anchor groups in the OPE derivatives. Further they have established that the increase in pendant unit conjugation of OPE derivatives would lead to a decrease in the Seebeck coefficient[34].

[5] *Martin Sebastian Zöllner et al* in 2021, have studied the potential of different radical substituents to induce spin polarization in electron transmission through OPE wires by means of first-principles DFT calculations in the coherent tunneling regime. They reported that the substituents' effects on overall transmission are minor when it comes to shifting up or down the energy scale. The main effect is a lowering of the

overall transmission minimum, which is, at least for verdazyl, caused by dispersion interactions between the substituents and the backbone, twisting one of the outer phenyl rings[35].

[6] *Yinqi Fan et al* in 2022, have studied the conductance and length dependence of amine and methyl sulfide-terminated oligo(phenylene ethynylene), and they have shown that the introduction of a graphene electrode leads to lower conductance values and attenuation factors, similar to what has been previously observed in alkane chains. They mentioned that this result is attributed to a shift of the electronic molecular levels toward the Fermi level, mainly driven by acetylene groups linking adjacent phenyl groups[36].

1.5. The Aims of the Study

The main aime of this thesis is to explore and understand the electric, thermoelectric, spectral and some of optical properties of molecular nano junction formed based on Oligo(phenylene-ethynylene) (OPE) Molecules. Also, it aims to understand the fundamentals and scientific facts that govern and control these properties. Finally, it tries to specify the possibility of utilizing these molecules in the field of optoelectronics applications.

Chapter Two

Density Functional Theory and Transport Calculations

2.1. Density Functional Theory

The Density Functional Theory (DFT) is widely used by physicists and chemists to investigate the ground-state properties of interacting many-particles systems such as atoms, molecules and crystals. DFT transforms the many-body system into one of non-interacting fermions in an effective field. In other words, the electrical properties of many interacting particles system can be described as a functional of the ground-state density of the system [37]. In 1998, the importance of DFT was confirmed with the Nobel Prize in Chemistry being awarded to Walter Kohn for his development of density functional theory. DFT is a reliable methodology which has been applied to a large variety of molecular systems with a huge number of books and articles in the literature giving detailed descriptions of the principles of DFT and its application [38-39]. The beginnings of DFT were founded upon the Thomas-Fermi model back in the 1920s which provided the basic steps to obtain the density functional for the total energy based on wavefunctions [40-41]. Further improvement was made by Hartree, Dirac, Fock and Slater and nearly four decades after the Thomas-Fermi work. DFT was

then given a robust foundation by the Hohenberg-Kohn theorems and Kohn-Sham method [38, 39, 42-43].

2.2. Kohn-Sham Method and Self-Consistent Field

Kohn and Sham noticed that Hohenberg-Kohn theory is applicable to both interacting and non-interacting systems. As DFT avoids the interacting many particle problem. The non-interacting system has one great advantage over the interacting system as finding the ground-state energy for a non-interacting system is easier. In 1965, Kohn and Sham came up with the idea, that it is possible to replace the original Hamiltonian of the system by an effective Hamiltonian (H_{eff}) of the non-interacting system in an effective external potential $V_{eff}(\vec{r})$ which gives rise to the same ground state density as the original system. Since there is no clear recipe for calculating this, the Kohn-Sham method is considered as an ansatz, but it is considerably easier to solve than the non-interacting problem. The Kohn-Sham method is based on the Hohenberg-Kohn universal density [41,44, 45, 46]:

$$F_{H-K}[n(\vec{r})] = T_{int}[n(\vec{r})] + Eee[n(\vec{r})] \qquad (2.1)$$

The Hohenberg-Kohn functional for non-interacting electrons is reduced to only the kinetic energy. The energy functional of the Kohn-Sham ansatz $F_{K-S}[n(\vec{r})]$, in contrast to (2.1), is given by[40]:

$$F_{K-S}[n(\vec{r})] = T_{non}[n(\vec{r})] + E_{Hart}[n(\vec{r})] + \int V_{ext}(\vec{r})\ n(\vec{r})\, d\vec{r}$$

$$+E_{xc}[n(\vec{r})] \tag{2.2}$$

where T_{non} is the kinetic energy of the non-interacting system which is different than T_{int} (for interaction system) in equation (2.1), while E_{Hart} is the classical electrostatic energy or classical self-interaction energy of the electron gas which is associated with density $n(\vec{r})$. The fourth term E_{xc} is the exchange-correlation energy functional and given by[43]:

$$E_{xc}[n(\vec{r})] = F_{H-K}[n(\vec{r}) - \overbrace{\frac{1}{2}\int \frac{n(\vec{r}_1)n(\vec{r}_2)}{|\vec{r}_1 - \vec{r}_2|} d\vec{r}_1 d\vec{r}_2}^{E_{Hart}[n(\vec{r})]} - T_{non}[n(\vec{r})] \tag{2.3}$$

The first, second and third terms in the equation (2.3) can be trivially cast into functional form. In contrast, there is in general no exact functional form for E_{xc}. In the last couple of decades, enormous efforts have gone into finding a better approximation toE_{xc}. Currently, the functional can investigate and predict the physical properties of a wide range of solid state systems and molecules. For the last three terms in the equation (2.3),

we take the functional derivatives to construct the effective single particle potential $V_{eff}(\vec{r})$:

$$V_{eff}(\vec{r}) = V_{ext}(\vec{r}) + \frac{\partial E_{Hart}[n(\vec{r})]}{\partial n(\vec{r})} + \frac{\partial E_{xc}[n(\vec{r})]}{\partial n(\vec{r})} \quad (2.4)$$

Now, we can use this potential to give the Hamiltonian of the single particle[47]:

$$H_{K-S} = T_{non} + V_{eff} \quad (2.5)$$

By using this Hamiltonian, the Schrödinger equation becomes:

$$[T_{non} + V_{eff}]\Psi_{K-S} = E\Psi_{K-S} \quad (2.6)$$

Equation (2.6) is known as Kohn-Sham equation. The ground state density $n_{GS}^{K-S}(\vec{r})$ corresponds to the ground state wavefunction Ψ_{GS}^{K-S} which by definition minimizes the Kohn-Sham functional subject to the orthonormalization constraints $\langle\Psi_i|\Psi_j\rangle = \delta_{ij}$; it is found by a self-consistent calculation [39, 48, 49].

Density functional theory uses a self-consistent field procedure. For example, let us suppose that E_{Hart} and E_{xc} can be accurately determined. The problem is now that V_{eff} cannot be calculated until the correct ground state density is known and the correct density cannot be obtained from the Kohn-Sham wavefunctions until equation (2.6) is solved with

the correct V_{eff}. Therefore we solve this circular problem by carrying out a self-consistent cycle [38, 50, 51] as shown in figure 2.1.

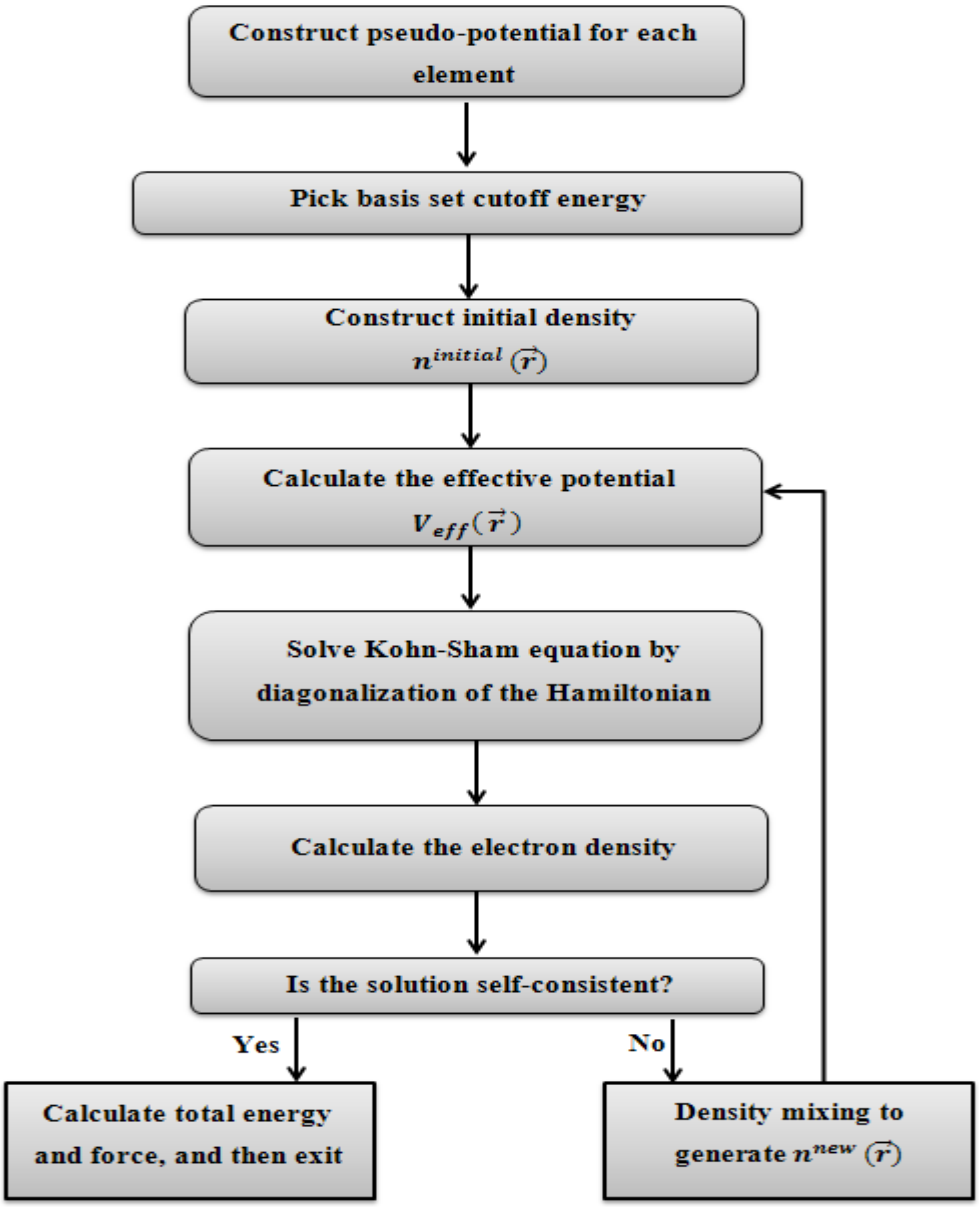

Figure 2.1. A Schematic illustration of the self-consistent DFT [51].

According to figure 2.1, the first step is to generate the pseudo-potential which represents the electrostatic interaction between the valence electrons and the nuclei and core electrons. The next step is to build the

required basis set with a selected kinetic energy cutoff to be inserted in the basis set; this step is to expand the density functional quantities. Clearly, if the density is known, the energy functional is fully determined. A trial electronic density $n^{initial}(\vec{r})$ is made as an initial guess. This initial guess is used to calculate the following quantity:

$$G = E_{Hart}[n^{initial}(\vec{r})] + E_{xc}[n^{initial}(\vec{r})] \tag{2.7}$$

Then $\frac{\partial G}{\partial n^{initial}(\vec{r})}$ and the effective potential V_{eff} are calculated. The effective potential is used to solve the Kohn-Sham equation (2.6) which leads to finding the electron Hamiltonian. After obtaining the Hamiltonian, it is diagonalised in order to find the eigenfunctions and the new electron density $n^{new}(\vec{r})$. Hopefully, this $n^{new}(\vec{r})$ will be closer to true ground state and is checked. For self-consistency, if this new updated electron density $n^{new}(\vec{r})$ agrees numerically with the density $n^{initial}(\vec{r})$ used to build the Hamiltonian at the beginning of the SCF cycle, we have reached the end of the loop. We then exit, and calculate all the desired converged quantities, such as the total energy, the electronic band structure, density of states, *etc*... Otherwise, the new density $n^{new}(\vec{r})$ does not agree with the starting density $n^{initial}(\vec{r})$, one generates a new input density and starts another SCF cycle: build the new density-dependent

Hamiltonian, solve and compute the density, and check for self-consistency [38, 52, 53].

The Kohn-Sham approach clearly shows that a complicated many body system can be mapped onto a set of simple non-interacting equations exactly if the exchange correlation functional is known. However, the exchange-correlation functional is not known exactly so approximations need to be made.

2.3. The Exchange-Correlation Aproximation

DFT is very reliable and proven method, but it still uses an approximation for the kinetic energy functional and the exchange-correlation functional in terms of the density. Huge efforts have been aimed at finding reliable expressions for those functional. The most commonly exchange-correlation functional approximations are the Local Density Approximation (LDA), which depends only on the density, and the more complicated Generalised Gradient Approximation (GGA), which includes the derivative of the density and also contains information about the environment and hence it is semi-local[52,53].

2.3.1. Generalized Gradient Approximation (GGA)

LDA treats all systems as the homogenous systems, but the real systems are inhomogeneous. In order to take this into account, a step may be taken beyond the LDA and extend it by including the derivative information of the density into the exchange-correlation functionals. The only way to do this, is by including the gradient and the higher spatial derivatives of the total charge density ($|\nabla n(\vec{r})|, |\nabla^2 n(\vec{r})|, ...$) into the approximation. Such a functional is called the generalized gradient approximation (GGA). For this case, there is no closed expression for the exchange part of the functional and therefore it has to be calculated along with the correlation contributions using numerical methods. Exactly as in the case of the LDA many parameterizations exist for the exchange-correlation energies in the GGA [54-55].

In this section, we are going to discuss the proposed functional form which is presented by **P**erdew, **B**urke and **E**rnzerhof (PBE) [54]. In this parameterization, there are two separated expressions, the first expression is the exchange $E_x^{GGA}[n(\vec{r})]$ and given by:

$$E_x^{GGA}[n(\vec{r})] = \int n(\vec{r})\, E_x^{homo}[n(\vec{r})]\, F_x(s) d\vec{r}\,, \qquad (2.8)$$

Where

$$F_x(s) = 1 + \kappa - \frac{\kappa}{(1+\mu s^2)/\kappa}$$

here $F_x(s)$ is called the enhancement factor, $\kappa = 0.804$, $\mu = 0.21951$ and $s = |\nabla n(\vec{r})/2k_s n(\vec{r})|$ is the dimensionless density gradient, where $k_s = \sqrt{\frac{4\,k_{T-F}}{\pi a_o}}$ and $k_{T-F} = \frac{(12/\pi)^{1/3}}{\sqrt{r_s}}$ is the Thomas-Fermi screening wavenumber whereas r_s is the local Seitz radius. The second expression is the correlation energy $E_x^{GGA}[n(\vec{r})]$ and given by:

$$E_c^{GGA}[n(\vec{r})] = \int (E_c^{homo}[n(\vec{r})] + \chi\,[n(\vec{r})])d\vec{r}\,, \qquad (2.9)$$

$$\chi\,[n(\vec{r})] = \frac{e^2}{a_o}\,\gamma\, ln\,\left(1 + \frac{\beta}{\gamma}\,t^2\,\frac{1+At^2}{1+At^2+A^2t^4}\right),$$

$$A = \frac{\beta}{\gamma}\,[\,e^{\left(\frac{E_c^{homo}{}_{[n(\vec{r})]}}{\gamma}\right)^{-1}}\,]^{-1}$$

where $\gamma = (1 - ln(2)/\pi^2$, $t = |\nabla n(\vec{r})/2k_{T-F}n(\vec{r})|$ is another dimensionless density gradient, $\beta = 0.066725$, and $a_0 = \frac{\hbar}{me^2}$.

LDA and GGA are the two most commonly used approximations for the approximation of exchange-correlation energies in the DFT. Also, there are several other functional, which go beyond LDA and GGA. In general, there is no robust theory of the validity of these functional. It is determined via testing the functional for various materials over a wide range of systems and comparing results with reliable experimental data.

2.3.2. Localised Atomic Orbital Basis Sets (LAOBs)

One of the most important aspects of the SIESTA code is the type of the basis function employed in the calculations. It uses a basis set composed of localised atomic orbitals which compare well with other DFT schemes which may use a plane wavefunction basis set [58]. The benefits from using LAOBs are that they provide a closer representation of the chemical bond; they can allow order-N calculations to be performed and also it gives a good base from which generate a tight-binding Hamiltonian. SIESTA uses confined orbitals, i.e. orbitals are constrained to be zero outside of a certain radius (cutoff radius r_c). This produces the desired sparse form of the Hamiltonian as the overlap between basis functions is reduced. The atomic orbitals inside this radius are products of a numerical radial function and a spherical harmonic. The simplest form of the atomic basis set for an atom (labelled as I) is called single-ζ (also called minimal) which represents a single basis function per electron orbital. It is given by the following equation, [59]:

$$\Psi^{\mathrm{I}}_{nlm}(\vec{r}) = R^{\mathrm{I}}_{nl}(\vec{r})\, Y^{\mathrm{I}}_{lm}(\vec{r}) \tag{2.10}$$

where $\Psi^{\mathrm{I}}_{nlm}(\vec{r})$ is the single basis function which consists of two parts, the first part is the radial wavefunction R^{I}_{nl} and the second part is the spherical harmonic Y^{I}_{lm}. Minimal or single zeta basis set are constructed

by using one basis function of each type occupied in the separate atoms that comprise a molecule. If at least one *p-type* orbital is occupied in the atom, then the complete set (*3p-type*) of the functions must be included in the basis set. For example, in the carbon atom, the electron configuration is $1s^2\ 2s^2\ 2p^2$, therefore, a minimal basis set for carbon atom consists of $1s, 2s, 2p_x, 2p_y$ and $2p_z$ orbitals which means the total basis functions are five as shown in table 2.1.

Higher accuracy basis sets called multiple-ζ are formed by adding another radial wavefunctions for each included electron orbital. Double basis sets are constructed by using two basis functions of each type for each atom. For carbon atom, a double zeta basis contains ten basis functions corresponding to ten orbitals which are $1s, 1s', 2s, 2s', 2p_x, 2p'_x, 2p_y, 2p'_y,$ $2p_z$ and $2p'_z$ [60]. For further accuracy, polarisation effects are included in double-ζ polarised basis sets obtained by including wavefunctions with different angular momenta corresponding to orbitals which are unoccupied in the atom [61]. A polarization function is any higher angular momentum orbital used in a basis set which is unoccupied in the separated atom. As an example, the hydrogen atom has only one occupied orbital type that is s-type. Therefore, if *p*-type or *d*-type basis functions were added to the hydrogen atom they would be known as polarization

functions. Carbon atoms with polarization functions include *d*-type and *f*-type basis functions.

Table 2.1. Examples of the radial basis sets functions per atom used in SIESTA code for different precisions of the split valence basis sets [62].

Atom/Basis Functions	Single-ζ (SZ)	Double-ζ (DZ)	Single-ζ Polarised (SZP)	Double-ζ Polarised (DZP)
$H^1/1s$	1	2	4	5
$C^6/1s\ 2s\ 2p_x 2p_y 2p_z$	4	8	9	13
$N^7/1s\ 2s 2p_x 2p_y 2p_z$	4	8	9	13

Assuming the core electrons (non-valence electrons) of an atom are less affected by the chemical environment than the valence electrons. This is so-called as split valence basis set. For example, the carbon atom, a split valence double zeta basis set would consist of a single $1s$ orbital, along with $2s, 2s'$ and $2p_x, 2p'_x, 2p_y, 2p'_y,\ 2p_z, 2p'_z$ orbitals, for a total of 9 basis functions. The basis functions in a split valence double zeta basis set are denoted $1s, 2s, 2s', 2p_x, 2p'_x, 2p_y, 2p'_y,\ 2p_z, 2p'_z$. In case of molecules, molecular orbitals can be represented as linear combinations of atomic orbitals (LCAO-MO) given by [63]:

$$\varphi_i(\vec{r}) = \sum_{v=1}^{L} a_{vi}\ \Psi_v(\vec{r}) \tag{2.11}$$

where φ_i represents the molecular orbitals (basis functions), Ψ_v are atomic orbitals, a_{vi} are numerical coefficients and L is the total number of the atomic orbitals.

2.4. Transport Calculations

2.4.1. Theoretical Building and Configuration

To get the structure of all systems in theory, have been utilized Avogadro programming. Avogadro is a propelled particle manager and visualizer intended for cross-stage use in computational science, molecular modeling, bioinformatics, materials science, and related areas (see figures 2.2 and 2.4). It offers flexible high quality rendering and a powerful plugin architecture [64]. Avogadro offers a semantic compound developer and stage for perception and investigation. For clients, it offers a simple to-utilize manufacturer, incorporated help for downloading from basic databases, for example, PubChem and the Protein Data Bank, separating synthetic information from a wide assortment of arrangements, including computational science yield [65].

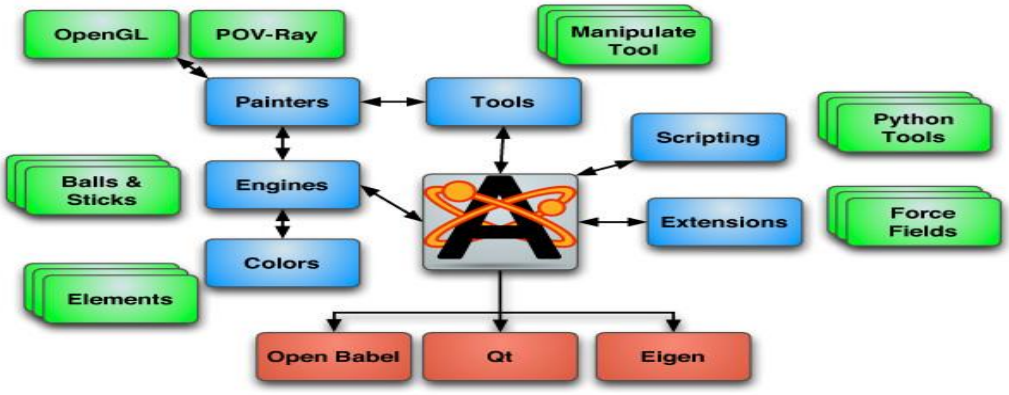

Figure 2.2. The abilities and tools of atomic building using Avogadro [66].

2.4.2. Optoelectronics Calculations

In the quest to better understand the trends in conductance behavior, the electronic, spectral, and some of optical properties of the molecules and the electrical behavior of the molecular junctions have been investigated by using density functional theory (DFT), and time-dependent density functional theory (TD-DFT) calculations. Initial studies carried out at the B3LYP level of theory [67] with 6-311G basis set [45-50]. Using these calculations the highest occupied and lowest unoccupied molecular orbitals (HOMO and LUMO, respectively) are investigated, and the emission strength oscillator (f_{em}), as shown in figure (2.3).

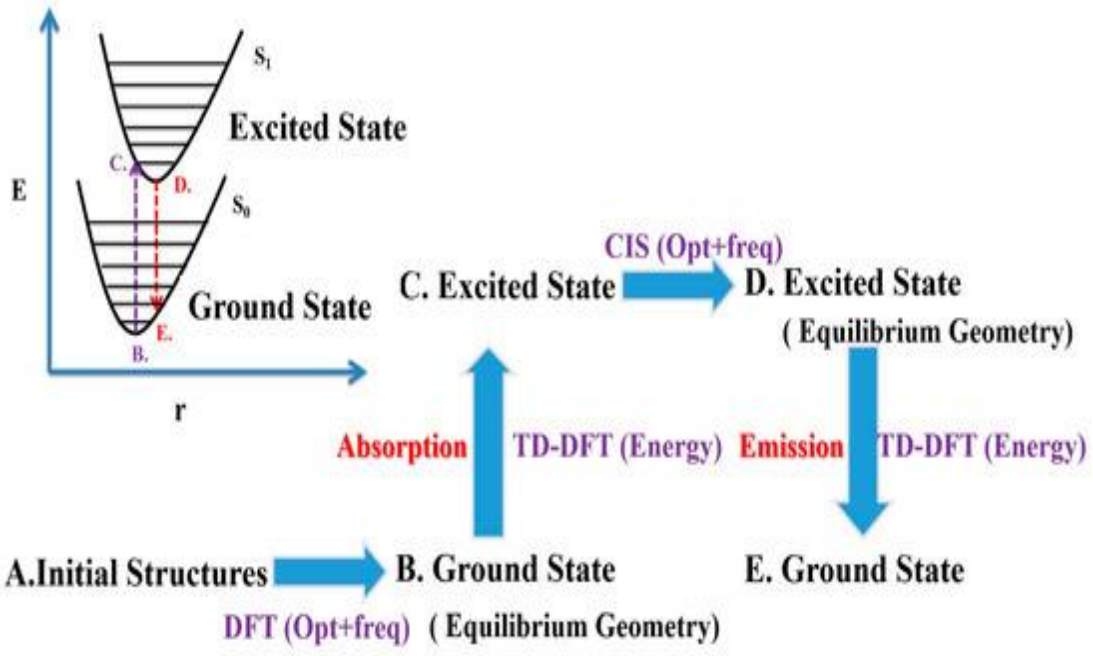

Figure 2.3. Steps of f_{em} calculations using DFT and TD-DFT methods [68].

2.4.3. Optimisation and Hamiltonian Calculations

All calculations in this thesis were carried out by the implementation of DFT in the SIESTA code. It is used to obtain the relaxed geometry of the discussed structures and also to carry out the calculations to investigate their electronic properties. SIESTA is an acronym derived from the ***S***panish *I*nitiative for ***E***lectronic ***S***imulations with ***T***housands of ***A***toms. It is a self-consistent density functional theory technique which uses norm-conserving pseudo-potentials and a **L**inear **C**ombination of **A**tomic **O**rbital **B**asis **s**et (LCAOB) to perform efficient calculations [69]. The SIESTA code is used to obtain the ground state energy, the corresponding Hamiltonian and overlap matrices of different atomic configurations, and then obtain the relaxed structure of the systems. This means that SIESTA can provide us the energy as a function of the atomic coordinates (position of atoms). The structure optimization (also known as geometry optimization) contains three options; relaxing atomic coordinates, allowing periodic cell shapes and volumes to change. In case of full optimization, the three options can be employed together, which leads to the minimum energy of the atoms in the system and the equilibrium lattice parameters of the systems. Performing the relaxation of the atomic positions allows atoms to move until the residual force between all atoms

is smaller than the required convergence tolerance in eV/Å as shown in Figure 3.3. In structural optimization the force is the key quantity and this force could be calculated numerically by taking the approximate numerical derivatives of the total energy with respect to the positions. This method is applied in SIESTA using the Hellmann-Feynman theorem [70]. Geometrical optimization of all molecules were carried out using the DFT code SIESTA, with a generalized gradient approximation (PBE functional), double-zeta polarized basis set, 0.01 eV/A force tolerance and a real-space grid defined with a plan wave cut-off energy of 250 Ry (see figure 2.4).

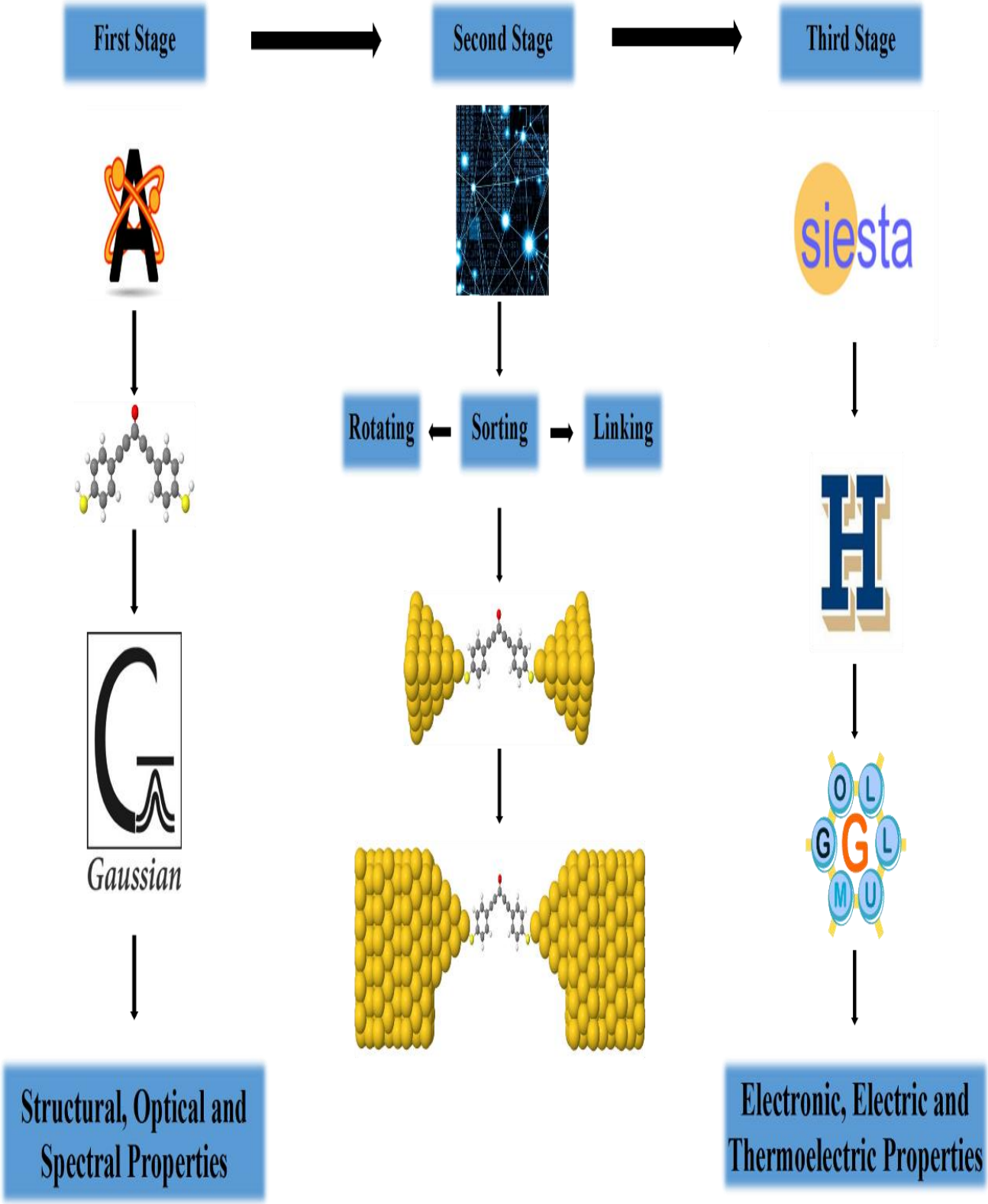

Figure 2.4. Steps of transport calculations.

2.4.4. Electric and Thermoelectric Calculations

To compute the electric and thermoelectric properties of molecules, they were each placed between pyramidal gold electrodes, then the molecule and first few layers of gold were again allowed to relax to yield the structures shown in the figure 2.5. For each structure, the transmission coefficient *T(E)* describing the propagation of electrons of energy *E* from the left to the right electrode was calculated by first obtaining the corresponding Hamiltonian and overlap matrices using SIESTA and then using GOLLUM code to compute *T(E)* via the relation [54]:

$$T = Trace\{\Gamma_R(E)G^R(E)\Gamma_L(E)G^{R\dagger}(E)\} \quad (2.12)$$

In this expression,

$$\Gamma_{L,R}(E) = i\left(\sum_{L,R}(E) - \sum_{L,R}{}^{\dagger}(E)\right) \quad (2.13)$$

describes the level broadening due to the coupling between left (L) and right (R) electrodes and the central scattering region, $\sum_{L,R}(E)$ are the retarded self-energies associated with this coupling and

$$G^R = (ES - H - \sum_L - \sum_R)^{-1} \quad (2.14)$$

is the retarded Green's function, where *H* is the Hamiltonian and *S* is the overlap matrix (both of them obtained from SIESTA) [57]. The electrical conductance *G(T)* and the thermopower *S* as a function of the temperature *T* was computed from the formula

$$l_n(T) = \int_{-\infty}^{\infty} dE(E - E_F)^n T(E) \left(-\frac{df(E)}{dE}\right) \quad (2.15)$$

Where

$$f(\mathrm{E}) = [e^{\beta(E-E_F)} + 1]^{-1} \quad (2.16)$$

is the Fermi function, $\beta=1/k_BT$, E_F is the Fermi energy, k is Boltzmann constant, T is the temperature. The electrical conductance $G(T)$ has been calculated by using Landauer formula [59]:

$$G(T) = G_\circ L_\circ(T) \quad (2.17)$$

where

$$G_0 = \left(\frac{2e^2}{h}\right) \quad (2.18)$$

Where go is the quantum of conductance, e is the charge and h is Planck constant. Since the quantity $(-\frac{df(E)}{dE})$ is a probability distribution peaked at $E=E_F$, with a width of order k_BT, the above expression shows that $G/G_\circ$ is obtained by averaging $T(E)$ over an energy range of order k_BT in the vicinity of $E=E_F$. Then, the thermopower S(T) is given by [59]:

$$S(T) = -\frac{L_1}{eTL_\circ} \quad (2.19)$$

2.4.5. Computational Programs

2.4.5.1. SIESTA Code

SIESTA (Spanish Initiative for Electronic Simulations with Thousands of Atoms) is an original method and its computer program implementation, to perform efficient electronic structure calculations and ab initio

molecular dynamics simulations of molecules and solids. SIESTA's efficiency stems from the use of strictly localized basis sets and from the implementation of linear-scaling algorithms which can be applied to suitable systems [57]. A very important feature of the code is that its accuracy and cost can be tuned in a wide range, from quick exploratory calculations to highly accurate simulations matching the quality of other approaches, such as plane-wave and all-electron methods.

2.4.5.2. Gollum Code

GOLLUM is a program that computes the charge, spin and electronic contribution to the thermal transport properties of multi-terminal junctions. In contrast to a non-equilibrium Green's function (NEGF) codes, GOLLUM is based on equilibrium transport theory, which means that it has a simpler structure, is faster, and consumes less memory. The program has been designed for user-friendliness and takes a considerable leap towards the realization of ab initio multi-scale simulations of conventional and more sophisticated transport functionalities [54].

The simpler interface of GOLLUM allows it to read model tight-binding Hamiltonians. Furthermore, GOLLUM has been designed to interface easily with any DFT code that uses a localized basis set. It currently reads

information from all the latest public flavors of the code SIESTA [71]. An interface to the code FIREBALL [72] is under development. These include functional that handle the spin–orbit or the van der Waals interactions or include strong correlations in the spirit of the local density approximation (LDA) approach. Plans to generate interfaces to other codes are underway. Two- and three-dimensional (3D) topological materials display fascinating spin transport properties. GOLLUM can simulate junctions made of these materials using either parametrized tight-binding Hamiltonians [73, 74] or DFT [75]. DFT does not handle correctly strong electronic correlation effects that are inherent in many nano-scale electrical junctions. As a consequence, a number of NEGF programs like SMEAGOL underestimate such effects. GOLLUM includes several tools to handle strong correlations. These include the above-mentioned interface to the versions of SIESTA containing the LDA+U functional. A second tool uses a phenomenological but effective approach called the scissors correction scheme. A third tool maps the DFT Hamiltonian into an Anderson-like Hamiltonian that is handled with an impurity solver in the spirit of dynamical mean field theory.

2.4.5.3. Gaussian Code

Gaussian is a very high-end quantum chemical software package, available commercially through Gaussian, Inc. The Software runs on virtually all computer platforms, including Microsoft Windows. In addition, it can be accessed through Web based, interface tools such as Web MO. Gaussian is the most powerful software available to, educators and student researchers through the North Carolina School Computational, Chemistry server. Currently, Gaussian09 (G09) is available. Figure 3.10 shows the flowchart of the Gaussian program. The "09" refers to the year 2009 in which the software was published. G09 is not the most recent version [76].

Chapter Three

Results and Discussion

A family of modified sulfur-functionalized Oligo(phenylene-ethynylene) (OPE) Molecules, as shown in figures 3.1, and 3.3 has been created to investigate their electronic, thermoelectric, spectral and some of optical properties.

3.1. Molecular Junctions Characteristics

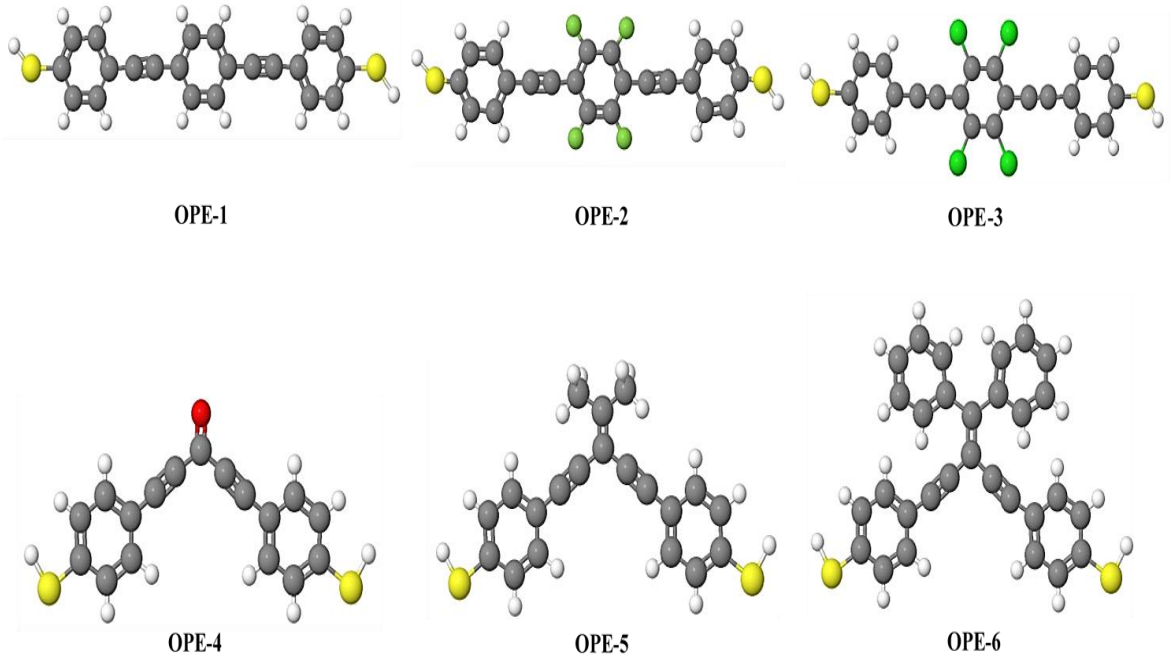

Figure 3.1. The optimized single molecules.

Table 3.1 : Type of molecules

Color	type
	Oxygen
	Carbon
	Fluorine
	Chlorine
	Hydrogen
	Sulfur

Chapter 3: Results and Discussion

The figure shows two groups of relaxed single molecules under study in this thesis. The structural aspects of these molecules are distinguished by various connections, since the first group has a para connection, while the second group has a meta connection. Secondly, the first group is characterized by a phenyl ring in the middle of molecule, whereas the second group is identified by single and double carbon-carbon bonds, respectively, linked to different side groups. On the other hand, there is another feature recognizes the molecules, which is the side structure of each molecule. Where OPE-1 with Hydrogen atoms (white atoms), while OPE-2 has Fluorine atoms (roughen green atoms). OPE-3 is featured by a Chlorine (shine green atoms), whereas OPE-4 is distinguished by a carbonyl functional group. The propene side groups is the characteristic of molecule OPE-5. Finally, OPE-6 molecule has two phenyl rings as a side group.

Table 3.2. The structural aspect of all molecules in contact with electrodes. L is the molecule length in contact with gold electrodes, which is the distance between Sulfur atoms (S…S). d is the distance between

Molecule	C–C (nm)	C=C (nm)	C≡C (nm)	C–S (nm)	C–O (nm)	C–F (nm)	C–Cl (nm)	C–H (nm)	L (nm)	d (nm)	X (nm)
OPE-1	0.143	0.139	0.121	0.175	-	-	-	0.109	1.997	2.242	0.245
OPE-2	0.143	0.139	0.121	0.175	-	0.133	-	0.109	1.997	2.242	0.245
OPE-3	0.143	0.139	0.121	0.175	-	-	0.176	0.109	1.997	2.242	0.245
OPE-4	0.141	0.138	0.119	0.179	0.122	-	-	0.109	1.448	1.693	0.245
OPE-5	0.141	0.138	0.119	0.179	-	-	-	0.109	1.448	1.693	0.245
OPE-6	0.141	0.138	0.119	0.179	-	-	-	0.109	1.448	1.693	0.245

Au…Au atoms. X is the bond length (Au…S).

Figure 3.1 and table 3.1 show there is an obvious difference in molecule length. Since, L of molecules with para connection is almost equals 2 nm, while molecules with meta have almost 1.45 nm molecule length. In addition, these results introduce a hint that these structures are π-conjugated molecules and they have an inner-shell electrons and σ-electrons are supposed to have their energies and distributions governed solely by the atomic orbital, or pair of orbitals, in which they move; and all effects depending on conjugation of unsaturation electrons, such as resonance energies and variations in bond order and electron density, are ascribed to the π-electrons.

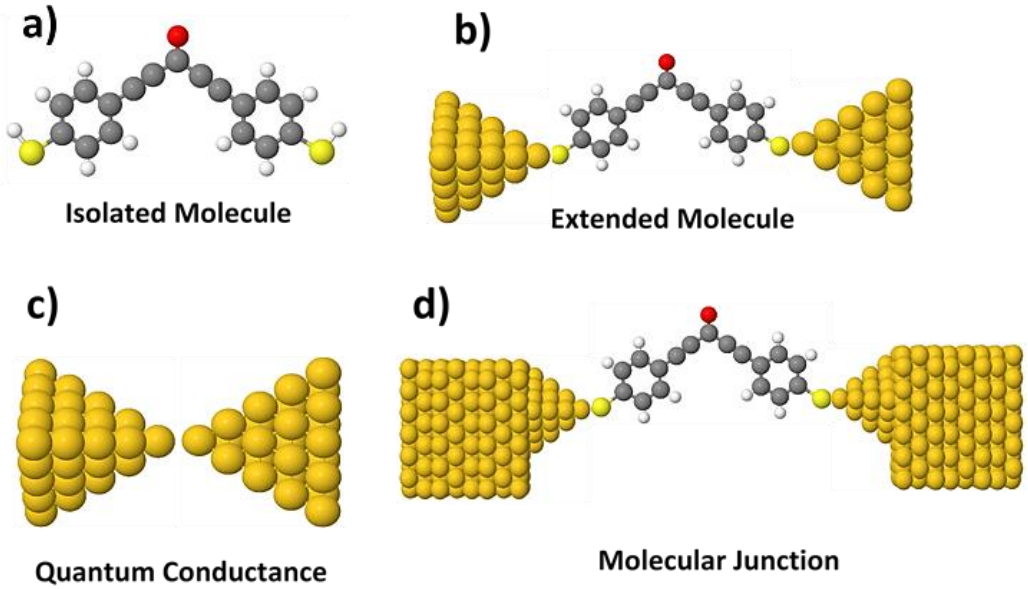

Figure 3.2. The optimized molecular junction of OPE-4, as an example. a) The relaxed single molecule; b) The optimized extended molecule; c) The relaxed pyramidal gold tips; d) The optimized molecular junction.

To provide further insight, and to better evaluate the properties and behavior of these molecular junctions, calculations using a combination of DFT and a nonequilibrium Green's function formalism were also carried out. Eight layers of (111)-oriented bulk gold with each layer consisting of 6×6 atoms and a layer spacing of 0.235 nm were used to create the molecular junctions, as shown in figure 3.3 and described in detail elsewhere [77].

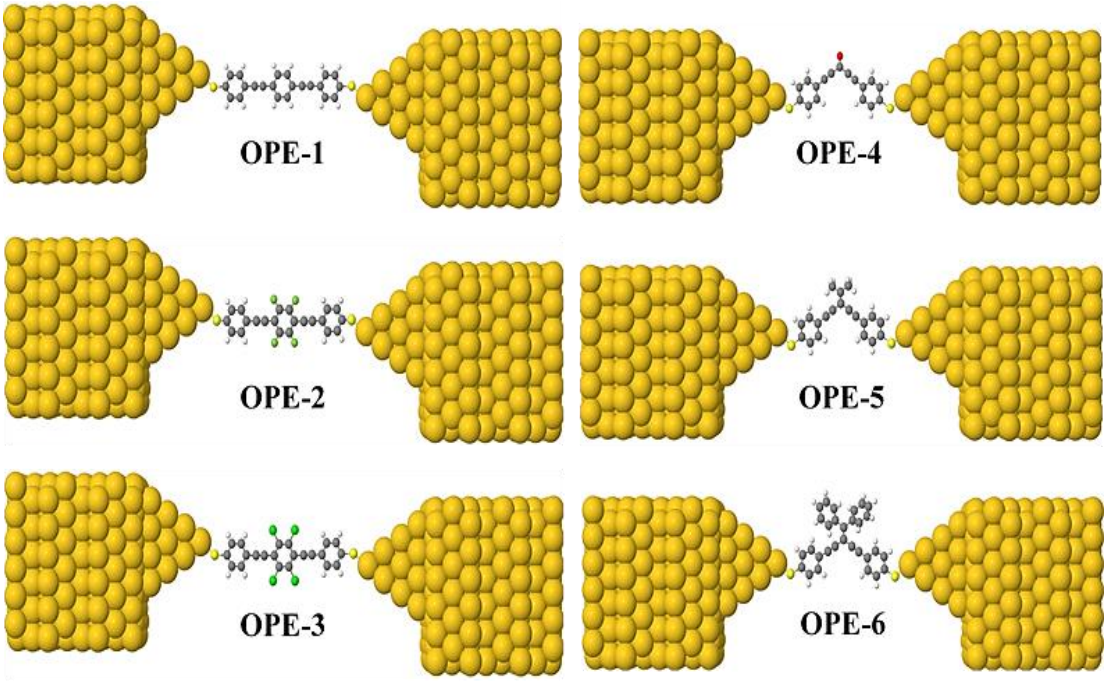

Figure 3.3. The optimized molecular junction of all structures.

The optimized molecular junction geometries conform well to a description of the thiol contacted compounds forming an angle of 52º

contact between the thiol anchor group and the undercoordinated gold atoms of the gold electrodes.

As expected, figure 3.3, and table 3.1 show that the thiol contacted compounds are oriented normal to the idealized pyramidal gold electrode surface within the molecular junction. Also, the molecular length of structures with para connection is longer than that of the compounds with meta connection.

3.2. Electric and Thermoelectric Characteristics

The most important result of figure 3.4a,b is the presentation of the relative

contribution to the conductance from quantum interference (QI) in the central part of molecules, and it demonstrates that the QI is satisfied at the level of DFT.

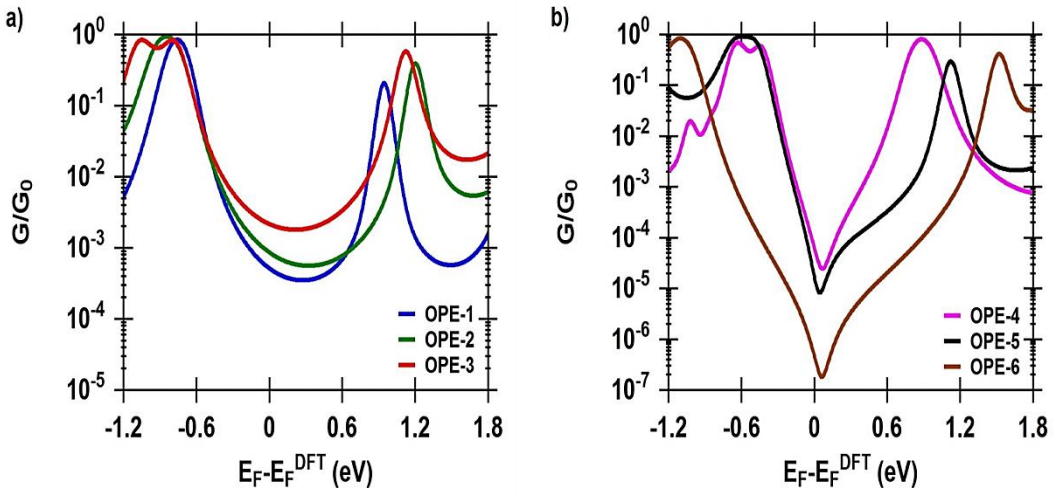

Figure 3.4. The electrical conductance of all structures.

Since, figure 3.4a,b demonstrates that for a wide range of Fermi energies, the conductances of the molecules with para connection (OPE-1,2,3) are distinctly higher than those of the molecules with meta connection (OPE-4,5,6), as expected from previous studies [78-81]. Additionally, figure 3.4a shows that molecule OPE-3 exhibited the highest electrical conductance, followed by molecule OPE-2, and then the lowest conductance is presented by molecule OPE-1. These results can be understood in terms of the number of electrons in the hybrid atom and their distribution over the shells. Where, OPE-3 possess chlorine atoms, and the atomic number of chlorine is 17, and its electrons configuration is $1s^2 2s^2 2p^6 3s^2 3p^5$. Hence, it has 2 electrons in its innermost shell, 8 electrons in its second shell and 7 electrons in the outermost shell respectively. While, OPE-2 has fluorine atoms that have 9 electrons, and electrons configuration $1s^2 2s^2 2p^5$. 2 electrons in a filled inner shell and 7 in an outer shell. Molecule OPE-1 has hydrogen atoms that have 1 electron. These results mean the number of electrons transferred from molecule (Γ) in OPE-3 is higher than that of OPE-2, which more than that of OPE-1, as shown in figure 3.5, and table 3.2. This could be a satisfy reason that the conductance order be as OPE-3 > OPE-2 > OPE-1. On the other hand, figure 3.4b shows an effect of different side groups on the value of the conductance. Since, the molecule OPE-4 has a carbonyl side

group and its conductance is higher than that of molecule OPE-5, which has a propene side group, and the conductance of this molecule is more than that of molecule OPE-6, which possess two phenyl rings. These results can be attributed to changing the path of the electrons while passing through these side groups, and the effect of parameters such as the rotation of phenyl rings in OPE-6, which leads to the lowest conductance. Finally, figure 3.4 also shows that for a wide range of energies in the gap between the HOMO and LUMO, the ordering of the conductance is OPE-3 > OPE-2 > OPE-1 > OPE-4 > OPE-5 > OPE-6.

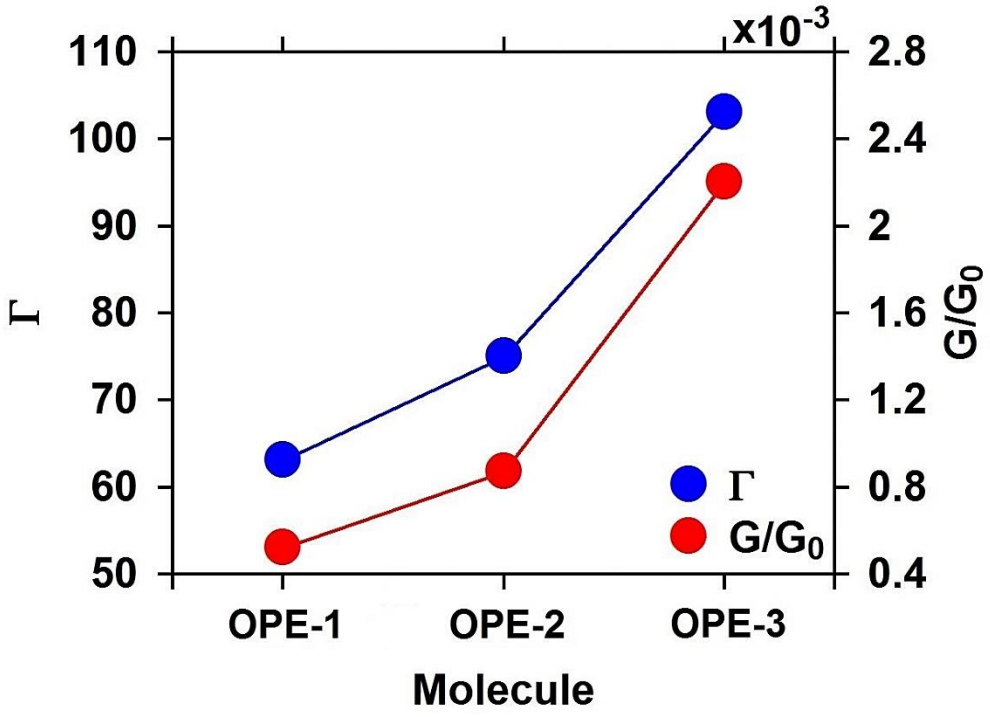

Figure 3.5. The transferred electrons from molecule to the electrodes (Γ), and the electrical conductance of OPE-1,2,3 molecular junctions.

To elucidate above results of the conductance, figure 3.5, shows a strong relationship between the number of electrons and the electrical conductance. In other words, high Γ leads to high G/G_0, and vice versa.

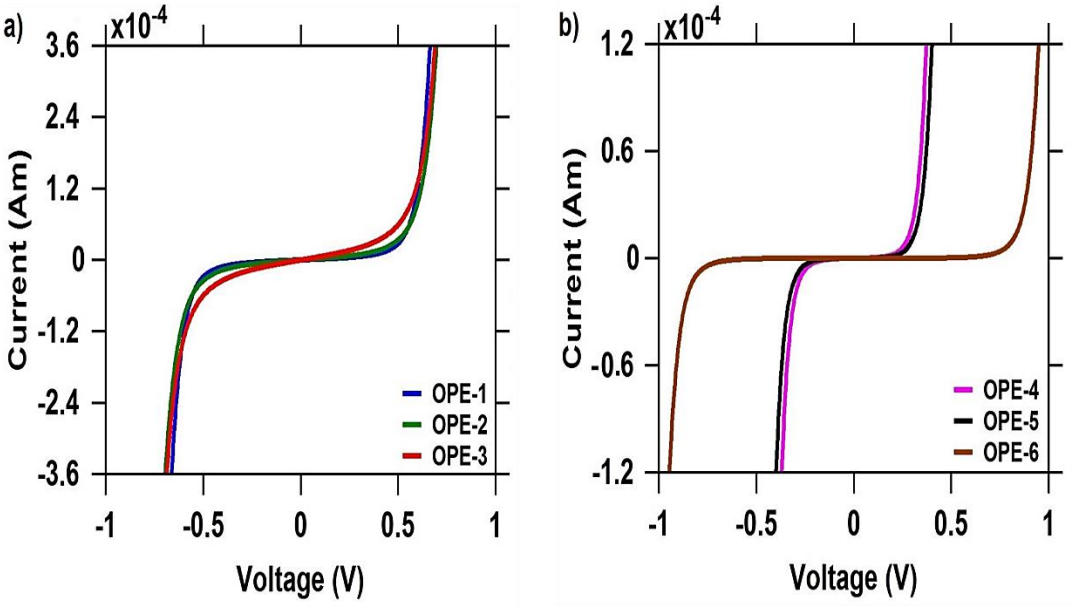

Figure 3.6. The current-voltage characteristics of all molecular junctions.

Primarily, figure 3.6 shows molecular junctions with current-voltage (I–V) characteristics curves which pass through the second quadrant, which means that they are active components, power sources, which can produce electric power. In addition, these results show threshold voltage (V_{th}), which is one of the most important physical parameters to determine and predicate the appropriate application, such as a field-effect transistor (FET), diodes and light emitting diodes. Threshold voltage is defined as the gate voltage at which the device starts to turn on. The accurate modeling of threshold voltage is important to predict correct circuit

behavior from a circuit simulator. Figure 3.6 predicates that the V_{th} of these molecular junction is between 0.5 V to 0.85 V (see table 3.2), which makes them perfect candidates for electronic and optoelectronic applications.

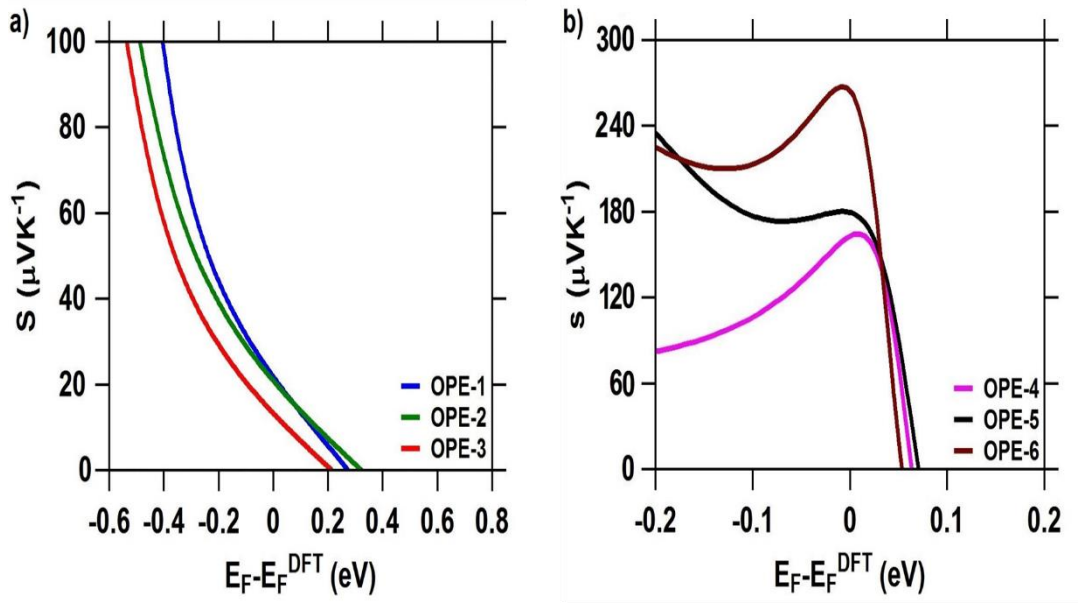

Figure 3.7. The thermoelectric of all molecular junctions.

Initially, these result could interpreted in terms of the phase of the interference, due different path ways of the wavelengths, which ascribed to para or meta connections. Therefore, an accurate explanation of these outcomes is the occurrence of destructive and/or constructive interferences.

Right hand panel of figure 3.7 shows also a promising strategy to enhance the thermopower using the destructive quantum interference. It is clear that meta connection in the medial of molecules leads to a destructive

interference, which in turn leads not only to a low electrical conductance value (as shown in figure 3.4, and table 3.2) for molecules with meta linking, but also a high value for the thermopower (S) of the structure itself. Since the molecule OPE-6 shows the lowest electrical conductance (0.17×10^{-6}), and the highest thermopower (266 μVK^{-1}). In contrast, the molecules OPE-3 introduces a highest conductance, which are 22×10^{-2}. At the same time this molecule presented the lowest S, which are 13 μVK^{-1} as shown in table 3.2. Another important result can be conclude from the figure 3.7, which is the sign of Seebeck coefficient S for all compounds is positive. This result suggests an important prediction that the transport mechanism is HOMO-dominated transport, which consistent with references [82-84]. Within the context, the quantum interference is not only specified the values order of electrical conductance and Seebeck coefficients as shown in figures 3.4 and 3.7, but also it was the crucial factor to develop the thermoelectric properties of molecular based devices. Finally, figure 3.7 demonstrates a result that the low conductance yields a high thermopower, and the quantum interference technique is a very powerful way to enhance and control the electronic and thermoelectric properties of molecular nano structures.

Table 3.3. The electrical conductance (G/G0). The thermopower (S). The threshold voltage (V_{th}). The transferred electrons (Γ).

Molecule	G/G_0	S μVK^{-1}	V_{th} V	Γ
OPE-1	0.52×10^{-3}	22	0.5	63
OPE-2	0.88×10^{-3}	21	0.5	75
OPE-3	22×10^{-2}	13	0.5	103
OPE-4	0.65×10^{-4}	165	0.3	-
OPE-5	0.5×10^{-6}	182	0.3	-
OPE-6	0.17×10^{-6}	266	0.85	-

3.3. Spectral and Optical Characteristics

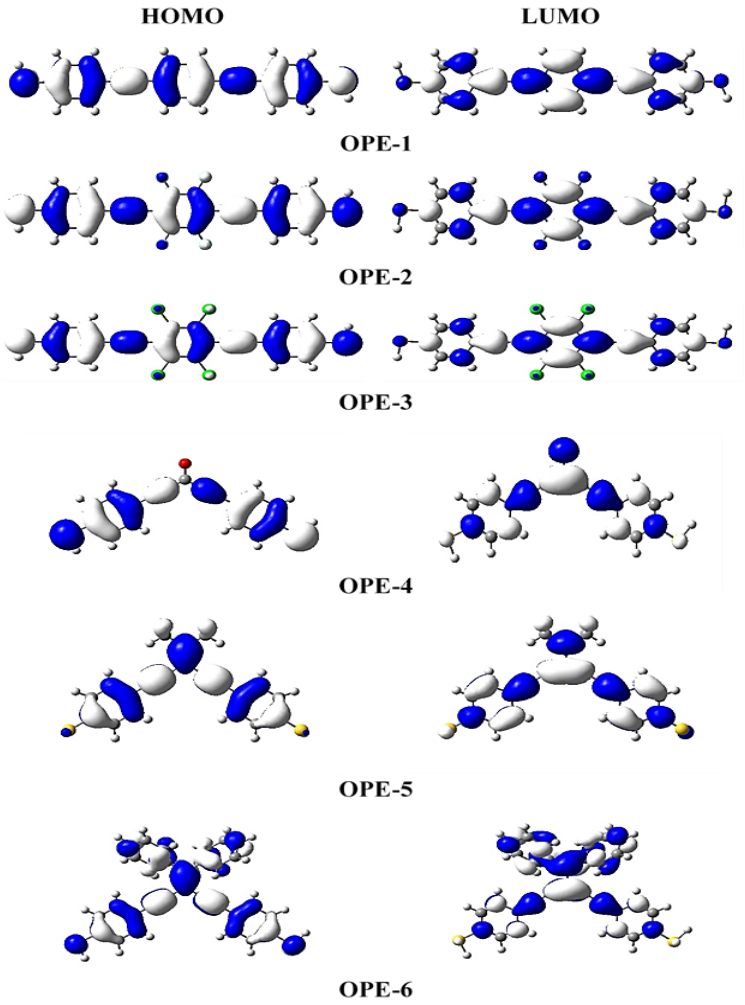

Figure 3.8. Represents the electronic structure and the distribution of the highest occupied molecular orbitals (HOMOs) and lowest unoccupied molecular orbitals (LUMOs) for all molecules.

Figure 3.8 shows the plots of iso-surface orbitals (HOMOs and LUMOs) for all molecules. Almost, density functional theory calculations have shown that the orbitals for both HOMO and LUMO of all molecules are extended through linear π interactions. Although, the weight of HOMO is nearly equals that of the LUMO, and this could be consider as a sign of the π-conjugation electrons transport in these molecules, but the HOMOs are concentrated on the C≡C bonds, while LUMOs are localized on the C–C bonds and shown less contribution than that of HOMOs. This could provide an additional evidence of the charge transport mechanism, which could be a HOMO-dominated transport, and consistent with results shown in figures 3.4 and 3.7. The results shown also a clear charge distribution and the contribution of HOMOs and LUMOs of the atoms Fluorine, Chlorine, and Oxygen atoms.

Table 3.3. The HOMOs and LUMOs energies. The HOMO-LUMO energies gap. The emission strength oscillator (f_{em}). The wavelengths (λ).

Molecule	HOMO (eV)	LUMO (eV)	H-L Gap (eV)	f_{em} (a.u.)	λ (nm)
OPE-1	- 0.75	- 0.94	1.69	2.15	352
OPE-2	- 0.85	- 1.20	2.05	2.15	390
OPE-3	- 0.80	- 1.11	1.91	2.03	400
OPE-4	- 0.63	- 0.88	1.51	0.96	372
OPE-5	- 0.60	- 1.11	1.71	0.75	252
OPE-6	- 1.10	- 1.51	2.61	0.66	411

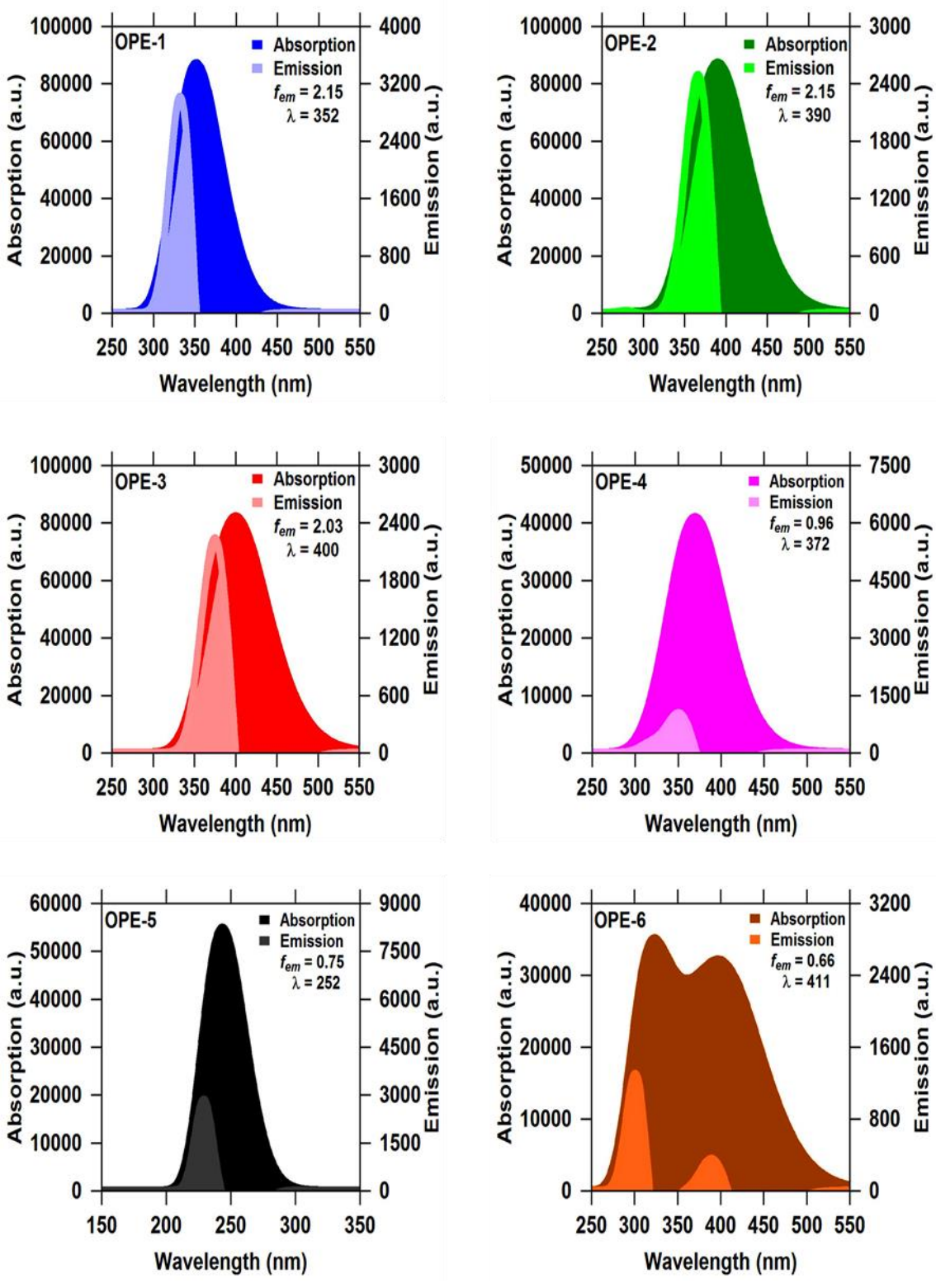

Figure 3.9. Represents the absorption, emission and emission oscillator strength of all molecules.

Chapter 3: Results and Discussion

Figure 3.9 presents the absorption and emission results for all the molecules under study in this thesis. Initially, it can be noticed that the emission intensity of the molecules characterized by the para connection is twice as high than those with meta connection. In fact, figure 3.9 illustrates that OPE-4,5,6 molecules have significantly smaller f_{em} (< 1) than other molecules. It is well known that the light amplification from these structures at room temperature will be difficult, which consistent with previous studies [85]. Since, the calculated emission cross section σ_{em} of a laser transition is consider an important parameter in a laser gain medium. It can affect laser performance in terms of threshold energy, output energy, maximum gain, etc. Under conventional lasing mechanism, a large σ_{em} is a prerequisite of a good laser gain medium [86]. Theoretically, for a given photoluminescence (PL) material, σ_{em} is directly proportional to the emission oscillator strength fem via [86]:

$$\sigma_{em}(v) = \frac{e^2}{4\varepsilon_0 m_e c_0 n_F} g(v) f_{em} \qquad (3.1)$$

where e is the electron charge, ε_0 is the vacuum permittivity, m_e is the mass of electron, c_0 is the speed of light, n_F is the refractive index of the gain material, ν is the frequency of the corresponding emission, and $g(v)$ is the normalized line shape function with $\int g(v)\, dv = 1$.

According to the aforementioned facts, OPE-4,5,6 molecules have much smaller f_{em}, which directly leads to small σ_{em}, and therefore any of these materials is not possible to serve as a good optical gain medium in practice. This result predicates a fact that the molecules with good thermoelectric properties (see figure 3.7 and table 3.2), possess a lower fluorescence (see figure 3.9 and table 3.3), and hence they are not good laser gain media, which is consistent with references [87-89].

On the other hand, molecules with para linking have a good emission oscillator strength (f_{em}), since they owned $f_{em} \approx 2$, and that means those structures are promising candidates for laser gain medium. In addition, molecules OPE-1, 2, 3 produce the maximum emission at wavelength between 350 nm and 400 nm, which in the visible region. This result bring us to an important result that those molecules could be powerful for the optoelectronic applications such as light emitting diodes.

Chapter Four

Conclusions and Future Works

4.1. Conclusions

This thesis includes theoretical study of the electrical conductance, thermopower and emission oscillator strength of a family of OPEs with thiol linker groups, with different transport connection para and meta. Various side groups such as phenyl rings or a carbonyl functional group or propene side groups were distinguish structural aspects of molecules.

The conductance results showed well-defined conductance features of the junctions formed. Where, the presentation of the relative contribution to the conductance from quantum interference (QI) in the central part of molecules, and it demonstrates that the QI is satisfied at the level of DFT. It can be conclude that the QI is a powerful strategy to control and enhance the conductance and thermopower. For a wide range of Fermi energies, the meta connection in the medial of molecules leads to a destructive interference, which in turn leads not only to a low conductance value (0.17×10^{-6}) for molecule OPE-6, but also a high value for the thermopower (266 μVK^{-1}) of this structure. In contrast, the molecule OPE-3 introduces a highest conductance 0.22 , and the lowest thermopower 13 μVK^{-1}. The sign of thermopower for all compounds is positive, which confirms another important conclusion, that the charge

transport mechanism is a HOMO-dominated transport. The OPE-4,5,6 molecules have much smaller f_{em}, (0.96, 0.75, and 0.66 respectively), which directly leads to small σ_{em}, and therefore it can be concluded that any of these materials is not possible to serve as a good optical gain medium in practice. Whereas, the molecules with para linking (OPE-1,2,3) have a good emission oscillator strength (f_{em}), since they owned $f_{em} \approx 2$, and that means those structures are promising candidates for laser gain medium.

In summary, it has been predicated employing a combined theoretical approaches, a rather uniform description of the formation and breaking of OPE-type molecular structures attached to gold electrodes. It has been demonstrated the role of the mechanical quantum interferences, and developed clear correlations between molecular structure features and electric, thermoelectric and spectral properties of these structures. This work shall serve as a guidance for future research on designing and developing nanoscale-based molecular circuits, such as light emitting diode, laser gain media and quantum switching devices.

4.2. Future Works

Molecular Nanotechnology is a field that can be consider a source of scientific and cognitive inspiration and innovation, so it could be suggested some of ideas for the future work as follows:

1- Study the phono transport characteristics of OPEs structures.
2- Investigation the optical and spectral properties of OPE-based molecules under magnetic field effects.
3- Study the quantum features of OPE families with different anchor groups.

References

References

[1] Moore, G.E., “Cramming more components onto integrated circuits”, McGraw-Hill, **1965**.

[2] Sarhan M. Musa, “Computational Nanotechnology: Modeling and Applications with MATLAB®”. CRC Press, **2011**.

[3] Bock, Charles W., Mendel Trachtman, and Philip George. "A Molecular orbital study of the rotation about the C D C bond in styrene", Chemical physics Vol. 93, No.3,p:p 431-443,**1985**.

[4] Davis, William B., Mark A. Ratner, and Michael R. Wasielewski. "Conformational Gating of Long Distance Electron Transfer through Wire-like Bridges in Donor− Bridge− Acceptor Molecules." Journal of the American Chemical Society Vol.123, No.32,p:p 7877-7886,**2001**.

[5] Nishizawa, Shohei, Jun-ya Hasegawa, and Kenji Matsuda, "Theoretical investigation of the β value of the π-conjugated molecular wires by evaluating exchange interaction between organic radicals" , The Journal of Physical Chemistry C ,Vol. 117, No.49, p:p 26280-26286, **2013**.

[6] De Cola, L. (Ed.), “Molecular Wires, From Design to Properties”, Topics in Current Chemistry, Springer: Berlin, Germany, Vol. 257 ,**2005**.

[7] Greaves, S. J., Flynn, E. L., Futcher, E. L., Wrede, E., Lydon, D. P., Low, P. J., & Beeby , A. "Cavity ring-down spectroscopy of the torsional motions of 1, 4-bis (phenylethynyl) benzene" , The Journal of Physical Chemistry A, Vol. 110, No.6 ,p.p. 2114-2121, **2006**.

[8] Diederich, François, Peter J. Stang, and Rik R. Tykwinski, eds, “Acetylene chemistry: chemistry, biology and material science”, John Wiley & KGaA, **2006**.

[9] He, J., Chen, F., Liddell, P. A., Andréasson, J., Straight, S. D., Gust, D., & Lindsay, S. M. ,” Switching of a photochromic molecule on gold

References

electrodes: single-molecule measurements. Nanotechnology “ , Vol.*16, No.* 6 , p.p. 695-702 , **2005**.

[10] Jenny, Nicolas M., Marcel Mayor, and Thomas R. Eaton. "Phenyl–Acetylene Bond Assembly: A Powerful Tool for the Construction of Nanoscale Architectures" , European Journal of Organic Chemistry , Vol. 2011 , No. 26 p.p. 4965-4983 , **2011**.

[11] Baumgardt, Ingmar, and Holger Butenschön. "1, 1′-Diaryl-Substituted Ferrocenes: Up to Three Hinges in Oligophenyleneethynylene-Type Molecular Wires", p.p. 1076-1087, **2010**.

[12] Aviram, Arieh, and Mark A. Ratner. "Molecular rectifiers" , Chemical physics letters , vol. 29, No. 2, p.p. 277-283,**1974**.

[13] Chen, Fang, Hihath, J., Huang, Z., Li, X., & Tao, N. J. , "Measurement of single-molecule conductance." Annu. Rev. Phys. Chem, Vol. 58 , p.p. 535-564 ,**2007**.

[14] McCreery, Richard L. "Effects of electronic coupling and electrostatic potential on charge transport in carbon-based molecular electronic junctions", Beilstein journal of nanotechnology , Vol. 7, No.1, p.p. 32-46 , **2016.**

[15] Moth-Poulsen, Kasper, and Thomas Bjørnholm , "Molecular electronics with single molecules in solid-state devices" , Nature nanotechnology , Vol. 4, No.9 , p.p. 551-556, **2009**.

[16] Cuevas, J. C.; Scheer, E., “ Molecular Electronics: An Introduction to Theory and Experiment” , World Scientific: Singapore, **2010**.

[17] van der Molen, Sense Jan, and Peter Liljeroth. "Charge transport through molecular switches", Journal of Physics: Condensed Matter , Vol. 22, No.13 , p.p. 133001-133030 , **2010** .

References

[18] Li, C., Mishchenko, A., Pobelov, I., & Wandlowski, T. , "Charge transport with single molecules–an electrochemical approach." CHIMIA International Journal for Chemistry, Vol. 64 , No. 6 , p.p. 383-390 , **2010**.

[19] Nichols, Richard J. , Haiss, W., Higgins, S. J., Leary, E., Martin, S., & Bethell, D. , "The experimental determination of the conductance of single molecules", Physical Chemistry Chemical Physics , Vol, 12 , No.12 , p.p. 2801-2815 , **2010.**

[20] Metzger, Robert M., ed. Unimolecular and Supramolecular " Electronics I: Chemistry and Physics Meet at Metal-Molecule Interfaces. Vol. 312. Springer Science & Business Media, **2012**.

[21] Tao, N. J. Nat. , " Electron transport in molecular junctions Nanotechnol" , Vol. 1 , No. 3, p.p. 173−181, **2006**.

[13] Song, Hyunwook, Mark A. Reed, and Takhee Lee. "Single molecule electronic devices." Advanced Materials , Vol. 23, No. 14, p.p. 1583-1608 , **2011**.

[22] Weibel, Nicolas, Sergio Grunder, and Marcel Mayor , "Functional molecules in electronic circuits." Organic & biomolecular chemistry , Vol.5 , No.15, p.p. 2343-2353,**2007**.

[23] Tour, James M. "Conjugated macromolecules of precise length and constitution. Organic synthesis for the construction of nanoarchitectures " Chemical reviews , Vol. 96, No.1, p.p. 537-554, **1996.**

[24] Díez-Pérez, Ismael, Hihath, J., Lee, Y., Yu, L., Adamska, L., Kozhushner, M. A. & Tao, N. . "Rectification and stability of a single molecular diode with controlled orientation", Nature chemistry , Vol.1, No.8, p.p. 635-641 , **2009**.

[25] Metzger, R. M., Chen, B., Höpfner, U., Lakshmikantham, M. V., Vuillaume, D., Kawai, T., ... & Ashwell, G. J. , " Unimolecular electrical rectification in hexadecylquinolinium tricyanoquinodimethanide" ,

References

Journal of the American Chemical Society ,Vol. 119, No.43 , p.p. 10455-10466, **1997** .

[26] Elbing, Mark, , Ochs, R., Koentopp, M., Fischer, M., von Hänisch, C., Weigend, F. & Mayor, M., "A single-molecule diode " , Proceedings of the National Academy of Sciences , Vol. 102, No. 25 , p.p. 8815-8820 , **2005**.

[27] Song, Hyunwook, Kim, Y., Jang, Y. H., Jeong, H., Reed, M. A., & Lee, T. "Observation of molecular orbital gating" , Nature , Vol. 462 , No.7276 , p.p. 1039-1043 , **2009.**

[28] Xu, Bingqian, Xiao, X., Yang, X., Zang, L., & Tao, N. , "Large gate modulation in the current of a room temperature single molecule transistor." Journal of the American Chemical Society , Vol. 127 , No.8 p.p. 2386-2387, **2005** .

[29] Lörtscher, Emanuel, Ciszek, J. W., Tour, J., & Riel, H. ,"Reversible and controllable switching of a single-molecule junction." Small Vol. 2 , No.8-9 , p.p. 973-977 , **2006** .

[30] Green, Jonathan E., Choi, J. W.; Boukai, A.; Bunimovich, Y.; Johnston-Halperin, E.; DeIonno, E.; Luo, Y.; Sheriff, B. A.; Xu, K.; Shin, Y. S.; Tseng, H.-R.; Stoddart, J. F.; Heath, J. R. "A 160-kilobit molecular electronic memory patterned at 1011 bits per square centimetre " Nature , Vol. 445 , No. 7126 , p.p. 414-417 , **2007**.

[31] Lee, Junghyun J., Chang, H., Kim, S., Bang, G. S., & Lee, H. "Molecular monolayer nonvolatile memory with tunable molecules" , Angewandte Chemie International Edition , Vol. 48 , No.45 , p.p. 8501-8504 , **2009**.

[32] Blum, A. Szuchmacher, and J. G. Kushmerick. "DP Long, CH Patterson, JC Yang, JC Henderson, Y. Yao, JM Tour, R. Shashidhar and

References

BR Ratna, “Molecularly Inherent Voltage-ControlledConductance Switching " , Nat. Mater , Vol. 4 , No. 2 , p.p. 167-172 , **2005** .

[33] Choi, Byoung-Young, Kahng, S. J., Kim, S., Kim, H., Kim, H. W., Song, Y. J. & Kuk, Y. "Conformational molecular switch of the azobenzene molecule: a scanning tunneling microscopy study " , Physical review letters Vol. 96 , No.15 , p.p. 156106 , **2006**.

[34] Quek, Su Ying, Kamenetska, M., Steigerwald, M. L., Choi, H. J., Louie, S. G., Hybertsen, M. S. & Venkataraman, L. , "Mechanically controlled binary conductance switching of a single-molecule junction" , Nature nanotechnology , Vol. 4 , No.4 , p.p. 230-234 , **2009** .

[35] van der Molen, Sense Jan, Liao, J., Kudernac, T., Agustsson, J. S., Bernard, L., Calame, M. & Schönenberger, C. "Light-controlled conductance switching of ordered metal− molecule− metal devices", Nano letters Vol. 9 , No.1 , p.p. 76-80 , **2009** .

[36] Argaman, Nathan, and Guy Makov , "Density functional theory: An introduction." American Journal of Physics, Vol. 68 , No.1 , p.p. 69-79 , **2000**.

[37] Dronskowski, R. “Computational chemistry of solid state materials : Wiley Online Library” , **2005** .

[38] Eschrig, Helmut , “The fundamentals of density functional theory” , Vol. 2. Leipzig: Edition am Gutenbergplatz, **2003**.

[39] Kohn, Walter, Axel D. Becke, and Robert G. Parr. "Density functional theory of electronic structure" , The Journal of Physical Chemistry , Vol. 100 , No. 31 , p.p. 12974-12980 , **1996** .

[40] Martin, Richard M. , “ Electronic structure: basic theory and practical methods” , Cambridge university press, **2020**.

[41] Parr, R.G. and Y. Weitao, “ Density-functional theory of atoms and molecules” , Oxford University Press, USA Vol. 16. **1994**.

References

[42] Kumar, Aditya. "A Brief Introduction to Thomas-Fermi Model in Partial Differential Equations " , **2012**.

[43] Lieb, Elliott H. "Erratum: Thomas-Fermi and related theories of atoms and molecules " , Reviews of Modern Physics , Vol. 54 , No.1 , p 311 , 1982.

[44] Gross, E.K. and R.M. Dreizler, " Density functional theory" , Springer Vol. 337. **1995**.

[45] Hohenberg, P.a.W.K., "Inhomogeneous Electron Gas. Physical Review" , Vol. 136 , No 3B **,** p.p. B864-B871 , **1964**.

[46] Kohn, W. and L.J. Sham, "Self-Consistent Equations Including Exchange and Correlation Effects" , Physical Review, Vol. **140** , No. 4A , p.p. A1133-A1138 , **1965 .**

[47] Levy, Mel. "Electron densities in search of Hamiltonians." Physical Review A , Vol.26 No, 3 , p1200 , **1982**.

[48] Eschrig, H., K. Koepernik, and I. Chaplygin. "Density functional application to strongly correlated electron systems", Journal of Solid State Chemistry , Vol.176 , No.2 , p.p. 482-495 , **2003** .

[49] Lima, N. A., L. N. Oliveira, and Klaus Capelle. "Density-functional study of the Mott gap in the Hubbard model." EPL (Europhysics Letters) , Vol.60 , No.4 , p. 601, **2002 .**

[50] Koch, Wolfram, and M. C. Holthausen. "A Chemist's Guide to Density Functional Theory, Wiley." Vol. 2 , **2001**.

[51] March, N. H., and R. Nesbet. "Self-Consistent Fields in Atoms", **1985** .

[52] Burke, K., the ABC of DFT, "Department of Chemistry" , University of California, **2007**.

References

[53] Kohn, Walter, and Lu Jeu Sham. "Self-consistent equations including exchange and correlation effects" , Physical review , Vol.140 , No.4A ,p. A1133 , **1965**.

[54] Perdew, J.P., K. Burke, and M. Ernzerhof, "Generalized gradient approximation made simple", Physical Review Letters, Vol. 77 No.18 , p.p. 3865-3868, **1996.**

[55] Becke, Axel D. "Density-functional exchange-energy approximation with correct asymptotic behaviour " , Physical review A , Vol. 38 , No.6 , p 3098 , **1988**.

[56] Hammer, B., L.B. Hansen, and J.K. Nørskov, "Improved adsorption energetics within density-functional theory using revised Perdew-Burke-Ernzerhof functionals" , Physical Review B, Vol. 59 , No.11, p. 7413,**1999**.

[57] Perdew, J.P. and Y. Wang, "Accurate and simple analytic representation of the electron-gas correlation energy" , Physical Review B, Vol. 45 No. 23 , p.p. 13244-13249 , **1992**.

[58] E. Artacho, J.D.G., A. Junquera, R. M. Martin, P. Ordejon, D. Sanchez-Portal, and J. M. Soler , " SIESTA 3.1" User's Guide. **2011**.

[59] Landauer, Rolf. "Spatial variation of currents and fields due to localized scatterers in metallic conduction" , IBM Journal of research and development , Vol. 1 , No.3 , p:p 223-231. **1957 .**

[60] Büttiker, M., Imry, Y., Landauer, R., & Pinhas, S. , "Generalized many-channel conductance formula with application to small rings." Physical Review B , Vol. 31 , No.10, p. 6207, **1985**.

[61] Datta, Supriyo , "Electronic transport in mesoscopic systems" , Cambridge university press, **1997**.

[62] Brouwer, P. W. "Scattering approach to parametric pumping " , Physical Review B , Vol. 58 , No.16, p. p. R10135-R10138, **1998**.

References

[63] Park, S., Wang, G., Cho, B., Kim, Y., Song, S., Ji, Y. & Lee, T. "Flexible molecular-scale electronic devices." Nature nanotechnology, Vol. 7 , No. 7, p.p. 438-442 , **2012**.

[64] Economou, E. N., and R. W. John. "Book-Review-Green's Functions in Quantum Physics " , Astronomische Nachrichten , Vol. 306 , p 340, **1985**.

[65] Mello, Pier A., and Narendra Kumar. "Quantum Transport in Mesoscopic Systems: Complexity and Statistical Fluctuations. A Maximum Entropy Viewpoint" , Oxford University Press, Vol. 4 , **2004**.

[66] Marcus D Hanwell, Donald E Curtis, David C Lonie, Tim Vandermeersch, Eva Zurek & Geoffrey R Hutchison, " Avogadro: an advanced semantic chemical editor, visualization, and analysis platform", Journal of Cheminformatics , Vol. 4 , No.1 , p.p. 1-17 , **2012**.

[67] Fisher, D.S. and P.A. Lee, "Relation between conductivity and transmission matrix". Physical Review B, Vol. 23 , No. 12 , p.p. 6851-6854 , **1981**.

[68] Huai-Wen Tsai, Kan-Lin Hsueh, Mei-Hsin Chen, Che-Wun Hong, "Electronic and Optical Properties of Polythiophene Molecules and Derivatives" , Crystals, Vol.11 , No.11, p:p 1292. 2021, **2021**.

[69] Visontai, D. "Quantum and Classical Dynamics of Molecule Size Systems " , Physics Department , Vol.2013, Lancaster University ,**2011**.

[70] Sanvito, Stefano, "Giant magnetoresistance and quantum transport in magnetic hybrid nanostructures" , Lancaster University (United Kingdom), **1999**.

[71] Finch, Christopher M. , "An understanding of the the electrical characteristics of organic molecular devices" , in Physics Department, Lancaster University, **2008**.

References

[72] Aoki, Hideo. "Real-space renormalisation-group theory for Anderson localisation: decimation method for electron systems" , Journal of Physics C: Solid State Physics, Vol. 13 , No. 18, p 3369 , **1980**.

[73] Lema, F., and C. Wiecko. "Multifractality of the Anderson and binary alloy localized eigenstates by the improved decimation method." Physica Scripta , Vol. 47 , No. 2 , p 129,**1993**.

[74] Leadbeater, M. and C.J. Lambert, "A decimation method for studying transport properties of disordered systems" , Annalen der physik, Vol. 7 , No.(5-6), p:p 498-502, **1998.**

[75] MacKinnon, J.G. and H. White, "Some heteroskedasticity-consistent covariance matrix estimators with improved finite sample properties" , Journal of Econometrics, Vol. 29, No. 3, p: p 305-325, **1985**.

[76] M. J. Frisch et al. Gaussian 03, Revision B.01. "Gaussian" Inc., Pittsburgh PA, **2009**.

[77] J Ferrer, C J Lambert, V M García-Suárez, D Zs Manrique, D Visontai, L Oroszlany, R Rodríguez-Ferradás, I Grace, S W D Bailey, K Gillemot, Hatef Sadeghi and L A Algharagholy , "GOLLUM: a next-generation simulation tool for electron, thermal and spin transport." New Journal of Physics , Vol.16 , No. 9, p . 93029 , **2014.**

[78] Aradhya, S. V., Meisner, J. S., Krikorian, M., Ahn, S., Parameswaran, R., Steigerwald, M. L. & Venkataraman, L. , "Dissecting contact mechanics from quantum interference in single-molecule junctions of stilbene derivatives." Nano letters , Vol.12 , No. 3, p.p. 1643-1647, **2012**.

[79] Arroyo, C. R., Tarkuc, S., Frisenda, R., Seldenthuis, J. S., Woerde, C. H., Eelkema, R., & Van Der Zant, H. S., "Signatures of quantum interference effects on charge transport through a single benzene ring " ,

References

Angewandte Chemie International Edition , Vol. 52 , No.11, p:p 3152-3155 , **2013**.

[80] Meisner, J. S., Ahn, S., Aradhya, S. V., Krikorian, M., Parameswaran, R., Steigerwald, M. & Nuckolls, C., "Importance of direct metal− π coupling in electronic transport through conjugated single-molecule junctions." Journal of the American Chemical Society , Vol. 134, p.p. 20440-20445 , **2012**.

[81] Arroyo, C. R., Frisenda, R., Moth-Poulsen, K., Seldenthuis, J. S., Bjørnholm, T., & van der Zant, H. S. , "Quantum interference effects at room temperature in OPV-based single-molecule junctions" . Nanoscale research letters, Vol. 8 , No. 1, p:p 1-6 , **2013**.

[82] Park, Y. S., Widawsky, J. R., Kamenetska, M., Steigerwald, M. L., Hybertsen, M. S., Nuckolls, C., & Venkataraman, L. , "Frustrated rotations in single-molecule junctions". Journal of the American Chemical Society, Vol. *131* , No.31 , p:p. 10820-10821 , **2009**.

[83] Hybertsen, M. S., Venkataraman, L., Klare, J. E., Whalley, A. C., Steigerwald, M. L., & Nuckolls, C., " Amine-linked single-molecule circuits: systematic trends across molecular families". Journal of Physics: Condensed Matter,Vol. *20* , No.37, p. 374115, **2008**.

[84] Bratkovsky, A. M., & Kornilovitch, P. E. , " Effects of gating and contact geometry on current through conjugated molecules covalently bonded to electrodes". Physical Review B, Vol. 67 , No.11, p.115307, **2003**.

[85] Ou, Q., Peng, Q., & Shuai, Z. , "Computational screen-out strategy for electrically pumped organic laser materials", Nature communications, Vol 11 , No.1 , p:p. 1-10 , **2020**.

[86] Nakanotani, H., Furukawa, T., Hosokai, T., Hatakeyama, T., & Adachi, C. , " Light amplification in molecules exhibiting thermally

References

activated delayed fluorescence". Advanced Optical Materials, Vol. 5 , No. 12, **2017**.

[87] Huang, H., Yu, Z., Zhou, D., Li, S., Fu, L., Wu, Y. & Fu, H. , "Wavelength-Turnable organic microring laser arrays from thermally activated delayed fluorescent emitters", Acs Photonics, Vol. 6 , No12 , p:p. 3208-3214 , **2019**.

[88] Ye, H., Kim, D. H., Chen, X., Sandanayaka, A. S., Kim, J. U., Zaborova, E. & Adachi, C., "Near-infrared electroluminescence and low threshold amplified spontaneous emission above 800 nm from a thermally activated delayed fluorescent emitter". Chemistry of Materials, Vol. 30 , No.19, p:p. 6702-6710, **2018**.

[89] Kim, D. H., D'aléo, A., Chen, X. K., Sandanayaka, A. D., Yao, D., Zhao, L. & Adachi, C. "High-efficiency electroluminescence and amplified spontaneous emission from a thermally activated delayed fluorescent near-infrared emitter" Nature Photonics, Vol.12, No.2, p:p. 98-104, **2018.**

الخلاصة

يعد التداخل الكمي (QI) أحد أكثر العلوم الأساسية، والذي يمكن أن يكون إستراتيجية قوية للتحكم في الخصائص الكهربائية والكهروحرارية والطيفية للجزيئات المفردة وتعزيزها. في هذا البحث تم استخدام حسابات النقل الكمومي القائمة على دالة الكثافة الوظيفية لمعرفة التوصيل الكهربائي (G/G_0)، والذي يوفر فهماً فريداً للقدرة الكهروحرارية (S) وقوى مذبذب الانبعاث (f_{em}) لسلسلة من مشتقات (*oligophenylene-ethynylene* (*OPE*)) مع مجموعات نهاية ثيول، وصلات التوصيل الالكتروني para أو meta، والتي تدعم خصائصها الكهروحرارية والبصرية والطيفية. أظهرت الجزيئات ذات الاتصال meta (6،5،OPE-4) توقيع تداخل كمي مدمر، مما أدى إلى توصيل كهربائي منخفض 0.65×10^{-4} و 0.17×10^{-6} و 0.5×10^{-6} على التوالي بالمقابل كانت القدرة الكهروحرارية لهذه التراكيب عالية $165\ \mu VK^{-1}$ و 182 و 266 وكذلك فان هذه الجزيئات انتجت قوى مذبذب انبعاث منخفضة للغاية 0.96 و 0.75 و 0.66 على التوالي. من الجانب الاخر، فان ارتباط para في الجزيئات 3،2،OPE-1 ادى إلى تداخل كمي بناء، والذي كان السبب الرئيسي للتوصيل الكهربائي العالي 0.22×10^{-2} و 0.52×10^{-3} و 0.88×10^{-3} على التوالى. بالنسبة للقدرة الكهروحرارية فقد كانت منخفضة جداً لهذه الجزيئات 22 و 21 و 13 وقوى مذبذب عالية الانبعاث عالية وهي 2.15 و 2.15 و 2.03 على التوالي. أخيراً, المدارات الجزيئية المشغولة العليا (HOMO) كانت المسوؤلة عن جميع خصائص النقل الكهربائي لهذه التقاطعات الجزيئية النانوية في هذه الدراسة.

جمهورية العراق
وزارة التعليم العـالي والبحث العلـمي
جامـــعة بـــابـــل
كليـــة العلـوم للبنات
قســـم فيزيـــاء الليزر

الخواص الكهروحرارية والبصرية للوصلات الجزيئية النانوية

رسالة مقدمة

الى مجلس كلية العلوم للبنات في جامعة بابل

وهي جزء من متطلبات نيل درجة الماجستير في علوم فيزياء الليزر وتطبيقاته

من قبل الطالبة

مروه عبد الحسين كاظم

بكالوريوس في علوم الفيزياء **(2016)**

بأشراف

أ.م.د. عدي اركان عباس الجبوري

١٤٤٣هـ **٢٠٢٢م**